Polym. Bull. (2010) 65:643–655
DOI 10.1007/s00289-009-0237-6

ORIGINAL PAPER

Novel branched poly(L-lactide) with poly(glycerol-*co*-sebacate) core

Shujun Cheng · Lijing Yang · Feirong Gong

Received: 25 September 2009 / Revised: 30 November 2009 / Accepted: 20 December 2009 /
Published online: 12 January 2010

Abstract A series of biodegradable poly (glycerol-sebacate-L-lactide) (PGSLA) copolymers, with variable PLLA length, were synthesized and characterized. The copolymers comprised PGS backbone chain with a nominal molecular weight of 2,800 g/mol. The length of each PLLA side chain covered the 800–14,000 range, while the length of the PLLA was easily controlled by the feed molar ratio of the L-lactide to the PGS. The structure of the copolymer was studied by nuclear magnetic resonance spectroscopy and gel permeation chromatography. Differential scanning calorimetric measurements and thermal gravimetric analysis had been performed to indicate the glass transition temperature (T_g), melting point (T_m), and the degree of crystallinity (χ_c). It was also found that the onset decomposition temperature (T_d) of the copolymers was lower than those of the linear polylactide (LPLLA). After solution casting and solvent evaporation, porous structures were found in the copolymer films by scanning electron microscope (SEM). Water contact angle results showed that the hydrophilicity of the copolymers was much higher than that of linear PLLA. In vivo, PGSLA copolymer demonstrated a favorable tissue response profile compared to PGS/LPLLA blend. There was also significantly less inflammation and fibrosis during degradation. PGSLA might therefore serve as an excellent candidate material for medical applications, given its minimal in vivo tissue response.

Keywords Polylactide · PGS · Branched · Copolymer

S. Cheng (✉) · L. Yang · F. Gong
Key Laboratory for Ultrafine Materials of Ministry of Education, School of Materials Science and Engineering, East China University of Science and Technology, Shanghai 200237, China
e-mail: chshj2003@yahoo.cn

Introduction

There has been growing concern about biodegradable polymers over the past two decades, especially in respect to their biomedical and pharmaceutical applications. Among the most promising have been synthetic biodegradable materials including polyesters as polyglycolid (PGA), polylactide (PLA), and poly (ε-caprolactone) (PCL). In fact, PLA has gained significant attention with respect to biomedical applications in surgery (e.g., surgical sutures, drug delivery systems, and internal bone fixation [1–4]), owing to the polymer's biocompatibility, biodegradability, and non-toxic nature. Most of the applications discussed above require the properties of PLLA to be modified, such as reducing the crystallinity or enhancing its hydrophilic property. This is achieved, for example, by copolymerization of ε-caprolactone, mesolactide, diglycolide, or other comonomers [5–8]. The introduction of branching to the PLA backbone is also proved to be one highly effective approach in tailoring the physical properties. Star-branched PLA has been investigated by numerous synthetic approaches [9–13]. Other types of branched PLA including comb-branched [14–19] and cross-linked [20, 21] structures have also received great attention.

The monomers of PGS polymers have the potential to be metabolized in vivo, as sebacic acid is a metabolite in fatty acid oxidation and glycerol is an intermediate in mammalian carbohydrate metabolism. Polyglycerol–sebacate–lactic acid (PGSL) with diverse feed ratios of glycerol, sebacate, and lactic acid, were synthesized, and the properties and mechanisms of the new polymer were investigated [22].

Until now, there have been a number of works published on copolymers with many shorter PLLA arms. These copolymers have unique properties, such as lower molecular weight distribution, better hydrophilicity, and faster biodegradation, compared to LPLLA with the same molecular weight. Most of the published works found that polyols are popular initiators as well as highly functional polymers. They attain hyperbranched or star shaped PLLA, such as pentaerythritol [13, 23–29], trimethylol propane [25–27, 30], polyglycerine [28], dipentaerythritol [30], di(trimethylol propane) [30], dendritic polyols [31–33], and so forth. However, most of the true initiators that functioned as the "cores" for preparation of star-shaped biodegradable PLLAs were non-biodegradable polyhydroxyl initiators or non-conducive natural products. Thus, after complete biodegradation of PLLA, the non-bioresorbable residual "core" compounds might be problematic, particularly for the specific in vivo applications.

In this article, the design of this polymer utilizes a kind of biodegradable multi-hydroxyl functional polyester as the initiator to obtain a series of branched PLLA with different arm-length to meliorate some properties of the PLLA, such as the strong hydrophobicity, poor cell affinity, high crystallinity, and difficulty in controlling polymer degradation. To realize the design, novel branch-shaped copolymers with PLLA side-arms and PGS back-bone have been synthesized and characterized. The objective of this study is to compare the material properties of these unique branched copolymers with those of linear PLLA, and their thermal and surface properties through the controllable arm-length of the copolymers.

Experimental

Materials

L-Lactide (97%), obtained from Purac, was recrystallized from toluene and dried under vacuum (70 mTorr) for 24 h prior to use; $Sn(Oct)_2$, purchased from Sigma, was fractionally distilled under vacuum (70 mTorr) and stored for short periods in sealed flasks under an nitrogen atmosphere at room temperature before use. Sebacic acid and glycerol were purchased from Sinopharm Chemical Reagent Co. Ltd. Before use, glycerol was distilled twice under reduced pressure and sebacic acid was purified by recrystallizing three times from anhydrous ethanol and dried under high vacuum at room temperature. The prepolymer of PGS was synthesized according to the previously published method of Wang et al. [34, 35] with some modification. All solvents were thoroughly dried and distilled before use.

Polymerization

Synthesis of PGS

The polymer was synthesized by polycondensation of an equimolar mixture of glycerol (Sigma) and sebacate (Aldrich) at 120 °C under nitrogen for 24 h before the pressure was reduced from 1 Torr to 40 mTorr over 5 h. Then, the reaction mixture was kept at 40 mTorr while heated to 140 °C and stirred for 8 h, under a constant flow of nitrogen gas. The resulting polymer features a small number of crosslinks and hydroxyl groups directly attached to the backbone.

Synthesis of poly (glycerol-sebacate-L-lactide) (PGSLA) copolymers

The PGSLA copolymer was synthesized by ring-opening polymerization (ROP) of L-LA initiated by the PGS. The PGS and L-LA were weighted into a 50 mL flame-dried, single-neck, round-bottom flask containing a Teflon-coated magnetic stir bar. Then 5 mg of $Sn(Oct)_2$ (0.5% of L-LA) was added as a 0.02 g/mL solution in dry dichloromethane. All the operations were carried out in a glovebox. After drying the monomer under vacuum and purging with dry nitrogen, the flask was flame-sealed and placed into an oil bath heated to 130 °C for 15 h. The obtained white polymer was dissolved into the dry dichloromethane and precipitated in methanol. After filtered, the precipitation was then dried in vacuum under room temperature.

Characterization

Gel permeation chromatography (GPC) The average molecular weights and polydispersity were determined by gel permeation chromatography (Waters HPLC system with Model 2690D separation module, Model 2410 refractive index detector and Shodex columns (K802.5, K803, and 805)).

Nuclear magnetic resonance spectroscopy (NMR) ^{1}H-NMR spectra were recorded at room temperature on a Bruker DRX-500 using $CDCl_3$ as the solvent

and the standard ($\delta = 7.26$ ppm). ^{1}H-NMR: 5.34–5.22 ($CH_2CH(OOR)CH_2OOC(CH)_8COO$); δ 5.22–5.10 ($OOCCH(CH_3)O$); 4.34–4.09 ($CH_2CH(OOR)CH_2OOC(CH)_8COO$); 2.42–2.25 ($CH_2CH(OOR)CH_2OOC(CH)_8COO$); 1.79–1.57 ($CH_2CH(OOR)CH_2OOC(CH)_8COO$); 1.56–1.42 ($CH_2CH(OOR)CH_2OOC(CH)_8COO$); 1.39–1.23 ($OOCCH(CH_3)O$).

Thermal analysis The glass transition temperature (T_g), the melting temperature (T_m), and the melting enthalpy (ΔH) were measured by DSC using a DSC2910 thermal analysis system under an inert nitrogen atmosphere. The thermograms ranged from 0 to 200 °C at 10 °C/min heating rate. Thermogravimetric analysis (TGA) was carried on a TGA2050 thermogravimetric analyzer (TA Instruments Inc., USA) at a heating rate of 20 °C/min from 30 to 500 °C under nitrogen atmosphere.

Water contact angle The samples used for observation were prepared by casting 1 (wt)% CH_2Cl_2 solution on a clean microscope cover-slide, and drying for 3 days at room temperature to remove the residual solvent. Then different contact angles of the copolymers were obtained by VCA Optima/VCA 3000S.

Scanning electron microscope The samples used for observation were prepared by casting 1 (wt)% CH_2Cl_2 solution on a clean microscope cover-slide and drying for 3 days at room temperature to remove the residual solvent. Surface morphologies of the polymer films were examined by using a scanning electron microscope (SEM, JSM-6360LV, JOEL).

In vivo tissue response The copolymers were dissolved in CH_2Cl_2 at a concentration of 10% (w/v) in the watch-glass. The copolymer films were obtained by evaporating the solution under room temperature and drying for 3 days to remove the residual solvent. Nude rats weighing 200–250 g were implanted with polymer films. Since the $PGSLA_7$ and $PGSLA_{20}$ fail to form films with particular strength, $PGSLA_{50}$ and PGS/LPLLA blend with the same composition of $PGSLA_{50}$ were implanted into the rats as controls. Animals with PGSLA or PGS/LPLLA implants were allowed to survive 7, 14, 28, and 42 days after implantation, and then killed via intramuscular pentobarbital overdose. The surgical wounds were re-opened; the leg musculature was removed en bloc with the polymer remnant, and fixed in 10% formalin for histological analysis. Specimens were prepared for H-E staining analysis.

Result and discussion

Polymerization of the PGSLA branched copolymer

The first step was to synthesize the PGS through bulk polycondensation reactions of the glycerine and sebacic acid monomers, as shown in Fig. 1. Figure 2a shows a typical ^{1}H-NMR spectrum of a PGS pre-polymer. The chemical composition of the pre-polymers was determined by calculating the ratios of the signal integrals of the glycerine to sebacic acid. PGS has abundant hydroxyl groups on its back-bone, which provides PGS with better hydrophilicity and faster biodegradation. According to the national titration standard, the acid value was determined, from which the

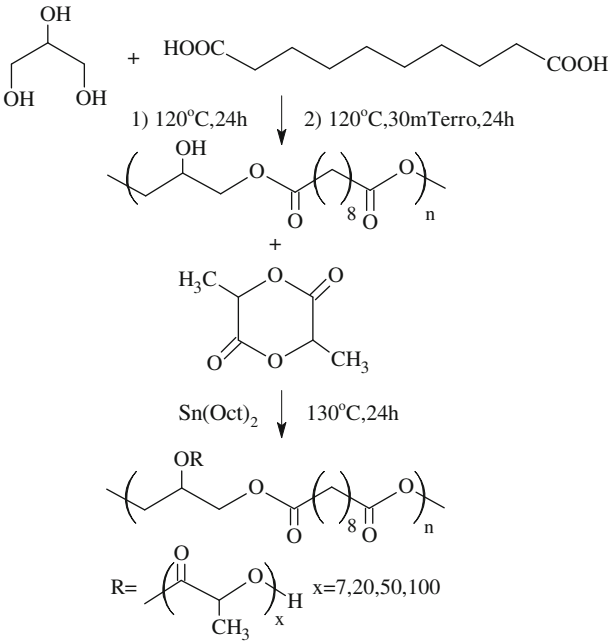

Fig. 1 Synthesis of copolymers

average hydroxyl number on the PGS back-bone was confirmed. Through acid value titration with KOH ethanol solution, it was discovered to have 11 hydroxyl groups for each PGS main chain. In addition, the number of average molecular weight (M_n) and polydispersity index (PDI) for PGS pre-polymer were determined by GPC, and are shown in Fig. 3.

In the second step in Fig. 1, the branched PGSLA copolyesters were prepared via the bulk copolymerization of L-LA and the PGS, using $Sn(Oct)_2$ as catalyst at 130 °C. Nevertheless, $Sn(Oct)_2$ does not initiate lactide ring openings alone. The addition of the hydroxyl groups forms a tin alkoxide which propagates ROP by an insertion coordination mechanism [36–39]. Since the tin alkoxide is the initiating species, the theoretical molecular weights of branched copolymers are dependent solely on average hydroxyl concentration of PGS relative to lactide. ^{1}H-NMR spectrum of the copolymer is illustrated in Fig. 2. The resonance of the (–HO–CH) groups of the PGS located at 3.93–3.61 ppm completely disappears (in Fig. 2a), while the signal integrals of the (–OOC–CH) groups at 4.34–4.09 ppm (in Fig. 2b) increase. This suggests that all of the hydroxyl on the PGS had participated in the ROP along with the $Sn(Oct)_2$. The polymerization of LA was carried out under rigorously anhydrous conditions to avoid any initiation by water, which will lead to a mixture of linear and branched copolymers.

The GPC curve of the copolymer in Fig. 3 remains symmetrical and monomodal, suggesting no linear PLLA was formed in the copolymerization. Narrow molecular weight distributions with PDI $= M_w/M_n$ values are typically lower than 2.0, as seen

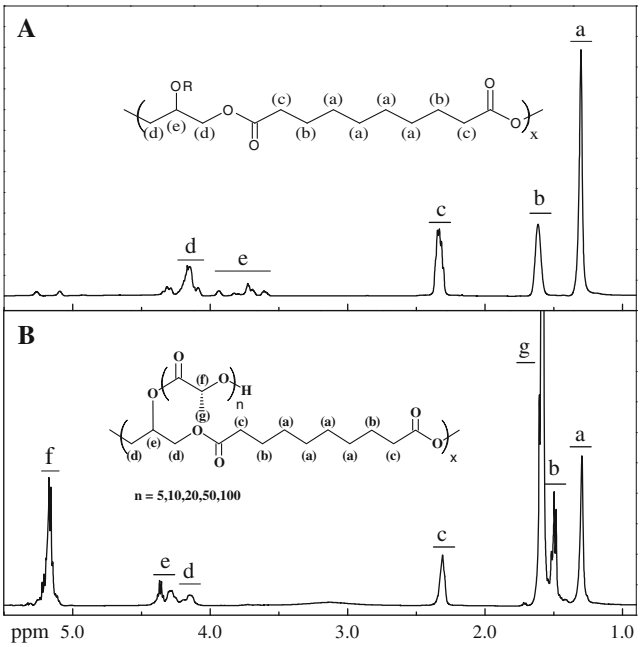

Fig. 2 Nuclear magnetic resonance spectroscopy (NMR)

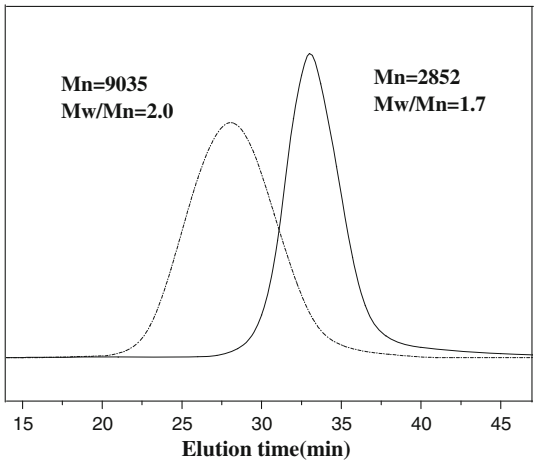

Fig. 3 GPC traces of PGS and PGSLA

in Table 1. These are observed for the final PGSLA products, as analyzed by GPC, which clearly shows how well the polymerization is controlled.

Table 1 shows that the GPC results correspond to four samples produced using various $[M]/[I]$ ratios. The molecular weight of the obtained copolymer increases linearly with the molar ratio $[LA]_0/[OH]_0$. This is consistent with the mechanism for alcohol-initiated ROP. The trend exhibits the dependence of molecular weight on initial hydroxyl concentration, as opposed to $Sn(Oct)_2$ concentration. This was the

Table 1 Molecular weight and water contact angel results of the copolymers

Sample	$[LA]_0/[OH]_0$	M_n[a]	M_n[b]	M_n[c]	M_w[c]	PDI
$PGSLA_7$	7	13888	11765	9035	27001	2.0
$PGSLA_{20}$	20	34480	30053	24457	53109	1.82
$PGSLA_{50}$	50	82000	77752	47513	85631	1.37
$PGSLA_{100}$	100	161200	145881	115531	169093	1.21

[a] Calculated from the free ratio, [b] calculated from ^{1}H-NMR spectrum, [c] obtained from GPC based on the PS calibration

same in each experiment. The theoretical molecular weights of linear polymers are dependent solely on hydroxyl mole relative to lactide, and are calculated as the following equation (assuming that all side hydroxyl groups initiate the ROP of LA (Eq. 1)):

$$M_n = \frac{[LA]_0}{[I]} 10 * M_{LA} x_{LA} + M_{PGS} \quad (1)$$

where $[LA]_0$ and $[I]$ are the feed molecular ratio of lactide and average hydroxyl side groups in the PGS, respectively. M_{LA} is the molecular mass of lactide, and the fractional conversion of lactide monomer x_{LA} equals 1, assuming that all terminal hydroxyl groups initiate the ROP of LA. The composition of the copolymers was determined using ^{1}H-NMR analysis and the ratio of representative peaks of the methylene. The PGS back-bone at 1.39–1.23 with the methine peaks was due to PLA at 5.25–5.15 ppm. In Fig. 4, the molecular weight of the obtained copolymer increases linearly with the molar ratio $[LA]_0/[OH]_0$, which is consistent with the mechanism for alcohol-initiated ROP.

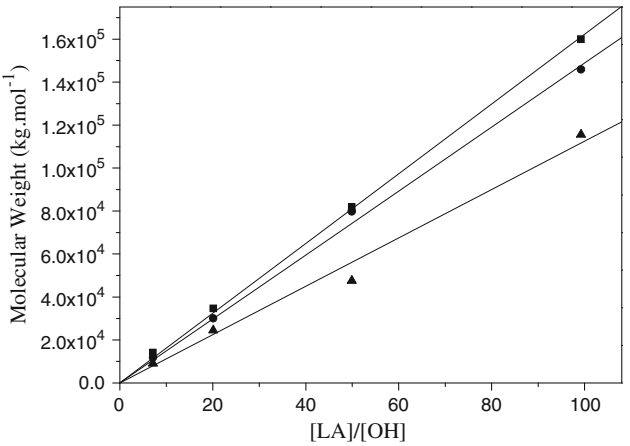

Fig. 4 Molecular weights as functions of the molar ratio of L-lactide (LA) monomer to the hydroxyl groups in PGS. *Filled square* M_n (theoretical), *Filled circle* M_n (NMR), *Filled triangle* M_n (GPC)

Thermal properties

Figure 5 shows the DSC curves of linear and PGSLA copolymers. The glass transition temperature (T_g), melting temperature (T_m), heats of fusion (ΔH_m), and crystallization enthalpy (ΔH_c) of copolymers were determined from DSC thermograms. The values estimated from Fig. 5 are shown in Table 2, together with the values of linear PLLA. Since there are two or more melting peaks observed in a DSC thermogram, the lowest melting peak is assumed as a real melting peak and other peaks are ascribed to the melting of the crystallites formed or thickened during DSC scanning.

From Fig. 5, it could be apparently found that both the melting and glassing temperatures tended to increase along with increasing molecular weight, indicating a tendency similar to those reported [40, 41]. The increasing molecular weight could be ascribed to the longer PLLA arms, which leads to a reduction in the mobility of the chains. On the other hand, the T_m and T_g of the copolymers are still lower than those of the linear PLLA with the same molecular weight. The reason being that the more arms of a branch-shaped PLLA would result in more chain-ends and shorten each arm length, accompanied with more densely packed chains near the PGS backbone, which finally creates imperfections in the ordered PLLA crystallites.

According to the values of ΔH_m and ΔH_c of PGSLA copolymers obtained from Fig. 5, the crystallization can be calculated as follows $\chi_c = (\Delta H_m - \Delta H_c)/H_m^0$ (the heat of fusion for 100% crystalline PLLA, $H_m^0 = 93.6$ J/g) [12, 42]. In comparison to the linear PLLA, the χ_c of the branch-shaped PLLA is relatively lower because of the plasticization of PGS and imperfect crystallinity in the branched structure. The χ_c increases proportionally with the length of PLLA arms and eventually approaches the value of LPLLA as the PLLA arms are sufficiently long, and the PLLA composition is dominant in the copolymers.

Thermal stability of the copolymers was analyzed by TGA. As shown in Fig. 6 and Table 2, the onset decomposition temperature (T_d) of the branched copolymer increases with the length of PLLA arms. The decreasing M_n of PGSLA can be

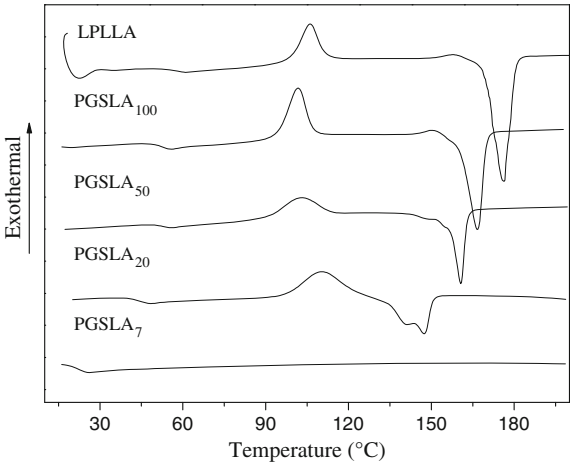

Fig. 5 DSC curves of copolymers with different molecular weights

Table 2 Thermal properties of copolymers

Sample	T_g (°C)	T_m (°C)	$\Delta H_m - \Delta H_c$ (J/g)	χ_c (%)	T_d (°C)	T_{max} (°C)	θ_{adv} (contact angle)
LPLLA	59.42	176.25	32.65	34.8	274	296	86
$PGSLA_7$	22.26	–	–	–	253	281	65
$PGSLA_{20}$	43.98	147.45	0.97	1.0	260	278	69
$PGSLA_{50}$	51.79	160.56	15.84	16.9	264	280	71
$PGSLA_{100}$	54.73	167.31	17.20	18.4	269	284	77

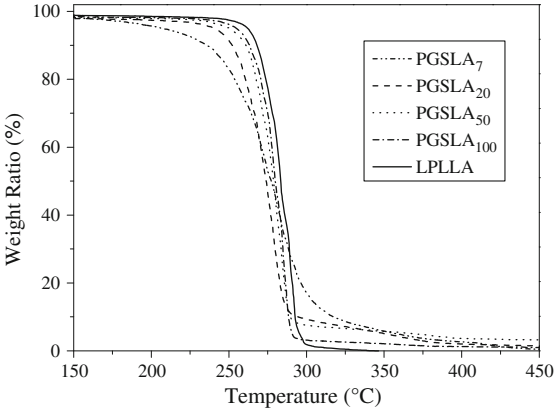

Fig. 6 TGA thermograms of LPLLA and PGSLA copolymers

ascribed to the enhanced chain mobility and increased number of terminal groups per unit mass (density of the terminal groups). These two factors increase the probability of back-biting or formation of lactides as volatile components. T_{max} determined from the maximum degradation rate peak in derivative thermogravimetry (DTG) thermograms (not shown) also increases with the molecular weight except $PGSLA_7$. It can be explained by a two-step decomposition process. The first step can be attributed to the decomposition of PLLA segments, while the second one is attributed to PGS segments. In $PGSLA_7$, the high density of thermal, unstable, terminal hydroxyl groups of PLLA chain and low-molecular weight led to a faster decomposition, forming cyclic monomer with a low T_d. For PGS, with a nominal-molecular weight of 2,800 g/mol, the value of T_d is 421 °C, which is much higher than the value of 274 °C for LPLLA. When the decomposition continues, the composition PGS center block, with a higher thermal stability, increases and consequently affects the tendency of the T_{max}.

Surface morphology and chemistry

Figure 7 shows the surface morphology of the branched copolymer film. PGSLA thin films were initially prepared by the solvent-cast technique of placing chloroform solutions onto polymers solution on glass slides, and evaporating the solvent directly at room temperature. At the $PGSLA_7$ surface, a smooth skin-layer is

observed (Fig. 7a) which is more dense (lower porosity) and has fewer pores, compared to the other three samples. The shape of the pores, in an ordered honeycomb structure in these skin layers, is approximately circular. Nevertheless, we failed to obtain any regularity of the diameters of the pores along the increasing length of the arms. The pore sizes and patterns were found to be regulated by a variety of influencing factors, such as the humidity of the surrounding-air, the concentration of the solution, the solvent properties etc. [43]. Water droplets were condensed on the cooling surface because of the rapidly evaporating solvent, and stabilized on the surface of the solution. As a result, only a layer of ordered pores was formed on the top of the surface of the films, while the underneath of the films was smooth and solid.

Like surface morphology, surface chemistry is another key factor in influencing cell responses. The surface hydrophobicities of the branched PLLA thin films were assessed by determining the advancing contact angle (θ_{adv}) with Milli-Q water. Figure 8 shows θ_{adv} versus the $[LA]_0/[I]$ ratio of the samples for thin films of PGSLAs with four types of molecular branches. With the increasing of the ratio, the θ_{adv} values of branched PLLA, to some extent, improved, respectively. The θ_{adv} values of PGSLA copolymer films presented a distinct change from 97° for $PGSLA_7$ to 115° for $PGSLA_{100}$. The resultant prolonged PLLA arms, which blanketed the ended-hydroxyl group of the other relatively shorter neighboring PLLA arms, were brought about by the less hydrophilic group on film surfaces. In contrast, the θ_{adv} value of the linear PLLA was relatively higher, indicating that the linear thin PLLA films, in comparison to the branched PLLAs, was thus less hydrophilic at the surface.

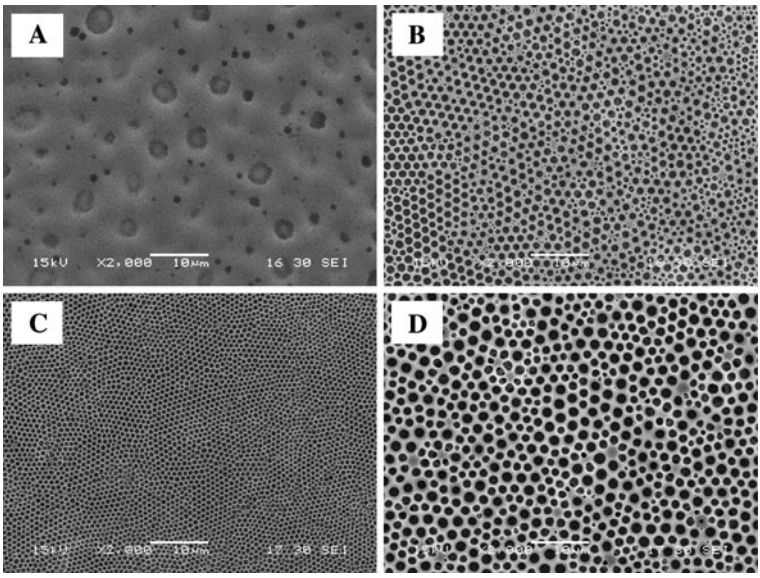

Fig. 7 SEM micrographs of PGS/PLLA copolymers. **a** $PGSLA_7$, **b** $PGSLA_{20}$, **c** $PGSLA_{50}$, and **d** $PGSLA_{100}$

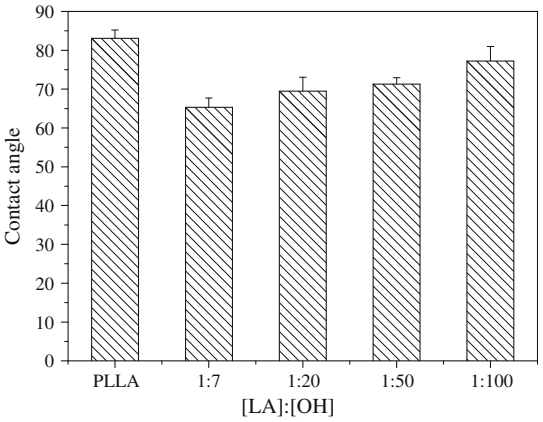

Fig. 8 Water contact angle of copolymer with different molecular weights

In vivo tissue response

The in vivo biocompatibility of PGSLA copolymers was evaluated via subcutaneous implantation in rats using the blending linear PLLA and PGS as the control. The appearance of the polymeric implants, and surrounding tissue, varied throughout the course of implantation. PGSLA copolymers and the PGS/LPLLA blend induced different early inflammatory responses, as assessed by fibrotic band thickness.

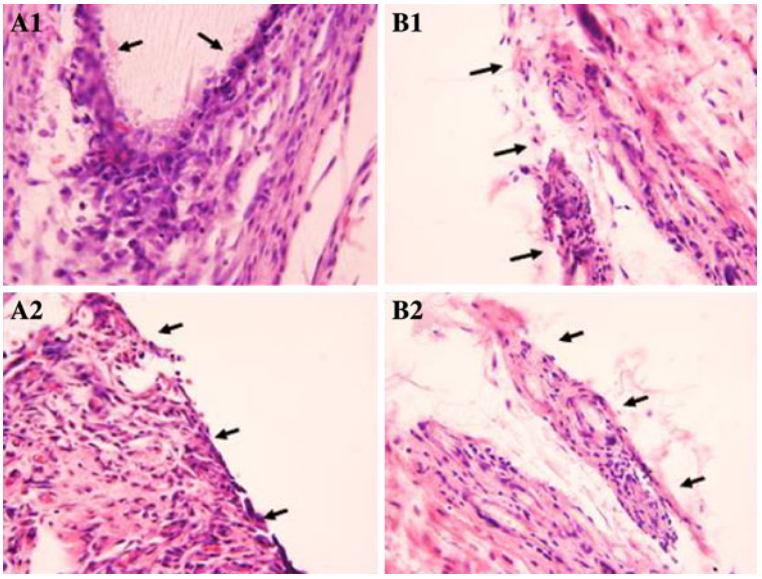

Fig. 9 In vivo biocompatibility. Porous PGS/LPLLA blend films and $PGSLA_{50}$ copolymer films were transplanted in nude rats. **a** After 2 week PGS/LPLLA blend films (a1, a2) showed a thicker inflammatory zone surrounding the films than $PGSLA_{50}$. Inflammation in the muscle (*arrowheads*) was found in PGSLA films. **b** After 4 weeks, the $PGSLA_{50}$ (b1, b2) inflammatory zone was reduced to comparable levels for PGS/PLLA blending films. Interface surfaces are denoted by *arrows*

The fibrotic zone thickness observations were strikingly different between the copolymer and blend samples. With the inflammation measures, PGS/LPLLA blend and PGSLA copolymer samples had similar fibrotic band thicknesses on day 14 (Fig. 9a1, b1). However, the observed thicknesses sharply diverged on day 28 (Fig. 9b1, b2). After 28 days in vivo, the acute inflammatory response was mild for the copolymers. The surrounding tissues did not show necrosis, or an abundant perivascular infiltration of mononuclear cells. The fibrotic band thicknesses decreased in copolymer at the remaining harvest points, while the thickness decreased slightly on day 28 and 42 in the blend samples.

Conclusions

This article established a one-pot method for bulk ring opening copolymerization of lactide with poly (glycerol-sebacate), changing the $[M]/[I]$ molar ratio to control the length of the PLLA side-chain. A series of PGSLA copolymers, with narrow molecular weight, were synthesized. The glass transition temperature (T_g), melting point (T_m), and crystallinity (χ_c) of the copolymer, systematically increased with the increasing arm length, while the corresponding values of the branched samples were still lower than the typical values of linear PLLA. With the increasing of the arm length, the hydrophilic property of the copolymer decreases. In addition, the surface of the branched copolymer film was porous and the structure was well-ordered. Through the in vivo cell response, the PGSLA has better biocompatibility than the PGS/LPLLA blend.

References

1. Vert M (1989) Angew Makromol Chem 166/167:155
2. Bendix D (1998) Polym Degrad Stab 59:129
3. Edlund U, Albertsson AC (2002) Adv Polym Sci 157:67
4. Stahelin AC, Weiler A, Rufenacht H et al (1997) Arthroscopy 13:238
5. Drumright RE, Gruber PR, Henton DE (2000) Adv Mater 12:1841
6. Kricheldorf HR (2001) Chemosphere 43:49
7. Okada M (2002) Prog Polym Sci 27:87
8. Albertsson AC, Varma IK (2002) Adv Polym Sci 157:1
9. Kim ES, Kim BC, Kim SH (2004) J Polym Sci B 42:939
10. Korhonen H, Helminen A, Seppälä J (2001) J V Polymer 42:7541
11. Biela T, Duda A, Penczek S et al (2002) J Polym Sci A 40:2884
12. Zhao YL, Cai Q, Jiang J et al (2002) Polymer 43:5819
13. Kim SH, Han YK, Kim YH et al (1992) Makromol Chem 193:1623
14. Barakat I, Dubois P, Jérôme R et al (1994) Polym Sci A 32:2099
15. Breitenbach A, Kissel T (1998) Polymer 39:3261
16. Eguiburu JL, Fernandez-Berridi MJ, San Roman J (1996) Polymer 37:3615
17. Jha S, Dutta S, Bowden NB (2004) Macromolecules 37:4365
18. Nouvel C, Frochot C, Sadtler V et al (2004) Macromolecules 37:4981
19. Ohya Y, Maruhashi S, Ouchi T (1998) Macromolecules 31:4662
20. Helminen A, Korhonen H, Seppälä J (2001) Polymer 42:3345
21. Storey RF, Warren SC, Allison CJ et al (1997) Polymer 26:6295

22. Sun ZJ, Wu L, Huang W et al (2008) Mater Sci Eng C 29:178
23. Kim SH, Han Y-K, Ahn K-D, Kim YH, Chang T (1993) Macromol Chem 194:3229
24. Lee S-H, Kim SH, Han Y-K, Kim YH (2001) J Polym Sci A 39:973
25. Dong CM, Qiu KY, Gu ZW, Feng XD (2001) Macromolecules 34:4691
26. Dong CM, Qiu KY, Gu ZW, Feng XD (2002) J Polym Sci A 40:409
27. Choi YK, Bae YH, Kim SW (1998) Macromolecules 31:8766
28. Korhonen H, Helminen A, Seppälä JV (2001) Polymer 42:7541
29. Finne A, Albertsson A-C (2002) Biomacromolecules 3:684
30. Biela T, Duda A, Rode K, Pasch H (2003) Polymer 44:1851
31. Gong FR, Cheng XY, Wang SF et al (2009) Polymer 50:2775
32. Zhao YL, Shuai XT, Chen CF, Xi F (2003) Chem Mater 15:2836
33. Atthoff B, Trollsås M, Claesson H, Hedrick JL (1999) Macromol Chem Phys 200:1333
34. Luo Y, Wang Y, Niu X, Shang J (2008) Eur Polym J 44:1390
35. Wang YD, Ameer GA, Sheppard BJ et al (2002) Nat Biotechnol 20:602
36. Gao J, Crapo PM, Wang YD (2006) Tissue Eng 12:917
37. Kowalski A, Duda A, Penczek S (1998) Macromol Rapid Commun 19:567
38. Penczek S, Duda A, Kowalski A et al (2000) Macromol Symp 157:61
39. Kowalski A, Duda A, Penczek S (2000) Macromolecules 33:689
40. Ioannis A, Atsuyoshi N, Norioki K et al (1995) Polymer 36:2947
41. Ioannis A, Atsuyoshi N, Eleni P et al (1996) Polymer 37:651
42. Cohn D, Younes H, Marom G (1987) Polymer 28:2018
43. Zhao BH, Zhang J, Wu HY et al (2007) Thin Solid Films 515:3629